International Journal of Innovative Computing, Information and Control
Volume **20**, Number **2**, April **2024**

ICIC International ©2024 ISSN 1349-4198
pp. **343–357**

HEALTH STATE PREDICTION OF S700K TURNOUT MACHINE BASED ON IMDE-SAE AND GAUSSIAN PROCESS REGRESSION

Wenjun Wei[1,2], Zheng Zhou[1,*], Mengyu Li[1] and Liben Yang[1]

[1]School of Automation and Electrical Engineering
[2]The Key Laboratory of Opto-Technology and Intelligent Control, Ministry of Education
Lanzhou Jiaotong University
No. 88, Anning West Road, Anning District, Lanzhou 730070, P. R. China
{ weiwenjun; lbyang }@mail.lzjtu.cn; 20203104110@stu.lzjtu.edu.cn
*Corresponding author: 11210431@stu.lzjtu.edu.cn

Received June 2023; revised October 2023

Abstract. *To fully exploit the health state information of S700K turnout machines and address the low utilization of existing power data and low prediction accuracy in turnout machine health assessment, this paper proposes a novel method for predicting the health status of turnout machines. The method combines the improved multi-scale dispersion entropy (IMDE), stack auto-encoder (SAE), and Gaussian process regression (GPR). Firstly, to overcome the issue of end information loss caused by traditional multi-scale dispersion entropy (MDE) during the construction of coarse granulation sequences, this paper applies a sliding time-shifted averaging method to obtaining multiple coarse granulation sequences within the same time scale. The average entropy value is then computed to obtain the IMDE value, which captures all the information of the sequence. The IMDE algorithm is applied to extracting the feature information of the power curve at multiple time scales, resulting in the IMDE feature vector of the turnout machine power curve. Next, the original signal is used as the input to the encoder of the SAE, while the IMDE feature vector serves as the corresponding label for the decoder. The one-dimensional output from the feature extraction layer of SAE is obtained as the health indicator (HI) of the turnout machine. Finally, the constructed HI dataset is split into training and testing sets, and a GPR model is trained to predict the state of the turnout machine. Through simulation validation and comparative analysis, the proposed IMDE-SAE-GPR model demonstrates improved prediction accuracy, providing scientific guidance for the preventive maintenance and health maintenance of turnout machines.*

Keywords: Multi-scale dispersion entropy, Stack auto-encoder, Gaussian process regression, S700K turnout machine, Health state prediction

1. **Introduction.** As one of the three major outdoor components of railway signaling equipment, the turnout machine plays a crucial role in ensuring smooth switching of the turnout, secure locking of the turnout, and real-time reflection of the turnout position. With the continuous development of China's railway transportation industry and the expansion of urban rail transportation construction, the S700K turnout machine has been widely deployed in various railway lines, imposing higher requirements on its safety and reliability [1,2]. Currently, maintenance strategies for turnout machines mainly involve regular inspections and post-failure repairs by railway authorities. This implies the need for periodic performance assessments of the turnout and emergency repairs following failures. However, this maintenance approach relies heavily on the expertise of maintenance staff and has the disadvantages of excessive maintenance and high safety risks [3]. To transform from reactive maintenance to proactive maintenance for turnouts, reduce

DOI: 10.24507/ijicic.20.02.343

maintenance costs, and minimize the occurrence of failures, it is necessary to employ a scientific approach to predict the real-time operational health status of turnout machines.

During the actual operation, the power curve of a turnout machine can, to some extent, reflect the current health condition of the equipment [4,5]. Numerous studies have been conducted to extract the features that reflect the degradation trend of turnout machines based on the power curves, and then to evaluate the health state of turnout machines. Zhong et al. [6] proposed a fault warning system for turnout machines by utilizing support vector data description (SVDD) to capture anomalous factors in the power curve. [7] employed the theory of local mean decomposition (LMD) and permutation entropy to extract the state features of turnout machines and achieve matching of the same operational states through fuzzy clustering. Wu and Chu [8] utilized wavelet packet decomposition to extract the state features of turnout machines and then applied Gath-Geva (GG) fuzzy clustering to classifying different degradation states. Zhang et al. [9] integrated adaptive white noise complete ensemble empirical mode decomposition (CEEMDAN) with kernel fuzzy c-means (KFCM) clustering to identify the degradation stages of turnout machines. The above methods obtained feature vectors characterizing the operating state of the turnout machines from different methods, but did not make further quantification of the health level. Moreover, the clustering-based approach is not sufficiently effective for the cases in different health state boundaries.

In this regard, some scholars construct turnout machine health state assessment models in an indicator-based manner [10-12]. Gao et al. [13] employed self-organizing map neural networks to reduce the dimensionality of temporal features of turnouts and capture their degradation trends. However, the subjective nature of selecting temporal features can introduce biases. Yin et al. [14] integrated empirical mode decomposition with fuzzy entropy theory to extract health indicators at various scales. Nevertheless, the choice of decomposition layers can impact the results. Zheng et al. [15] employed the Hausdorff distance to measure the similarity between the test curve and a reference library, thereby determining the health value of the turnout machines. However, this method relies on the construction of a rigorously defined reference library.

In recent years, dispersion entropy has been widely applied in the feature extraction of mechanical vibration signals, enabling the acquisition of more representative vectors at multiple time scales [16,17]. However, there is a problem of end information loss in the coarse granulation process. Auto-encoder is a self-supervised neural network model with a number of applications in the dimensionality reduction of high-dimensional nonlinear data [18,19]. As a nonparametric regression model, Gaussian process regression possesses a rigorous statistical foundation and exhibits good adaptability for regression prediction tasks in high-dimensional, nonlinear, and small-sample domains [20,21]. In light of these considerations, this paper proposes a method for predicting the health indicators of turnout machines based on improved multi-scale dispersion entropy, stack auto-encoder, and Gaussian process regression. The method quantitatively evaluates the health state of turnout machine through regression prediction, and the prediction effect is more accurate; at the same time, the corresponding feature extraction is carried out in a self-training way, which does not require the annotation of relevant data and the establishment of a standard library. By employing a sliding time-shifted averaging method at the same time scale, multiple components are constructed, and the average dispersion entropy is calculated to obtain the improved multi-scale dispersion entropy value without losing the original signal information, addressing the problem of end information loss. The stack auto-encoder combines the power signal and entropy features for dimensionality reduction, resulting in a one-dimensional health indicator for the turnout machine. Finally, a Gaussian process regression model is trained to predict the regression of the power curve and health indicator of the S700K turnout machine, establishing a predictive model for the health state of the turnout machine and providing scientific guidance for the health management of turnout machine in terms of operation and maintenance. In the first two sections of this paper, the current state of research and the working principle of turnout machine are presented. In Section 3, the basic principles of several algorithms used in the article are briefly explained. In Section 4, we sort out the experimental procedure of this study, and analyze the experimental results in Section 5. Finally, this paper summarizes the advantages of the proposed method for predicting the health status of turnout machine and provides an outlook on future research directions.

2. **The Turnout Conversion System of S700K.** The S700K turnout machine, produced by Siemens AG in Germany, is an advanced traction device widely employed in the construction of high-speed railways in China. As the primary actuator of railway turnouts, it serves the following functions:

1) Pushing or pulling the turnout to transition between the normal and reverse positions;

2) Locking the turnout after it has achieved precise alignment to prevent displacement due to external forces;

3) Providing real-time feedback on the position of the turnout, indicating its status;

4) Promptly issuing alarm notifications in case of malfunctions such as switch split.

Figure 1 shows the internal structure of an S700K turnout machine. The S700K turnout machine is powered by a three-phase asynchronous motor. During the process of turnout transition, there exists a relationship between the tension force F of its actuating lever and the output power P [7]:

$$F = \frac{9950}{rn\eta} P \tag{1}$$

In the equation, r, n and η represent the equivalent moment arm, rotational speed and motor efficiency of the S700K turnout's transmission system, respectively. It can be observed that there exists a certain linear relationship between the mechanical performance of the S700K turnout and the amplitude of its power curve. Thus, the power curve can, to some extent, reflect the operating state of the turnout.

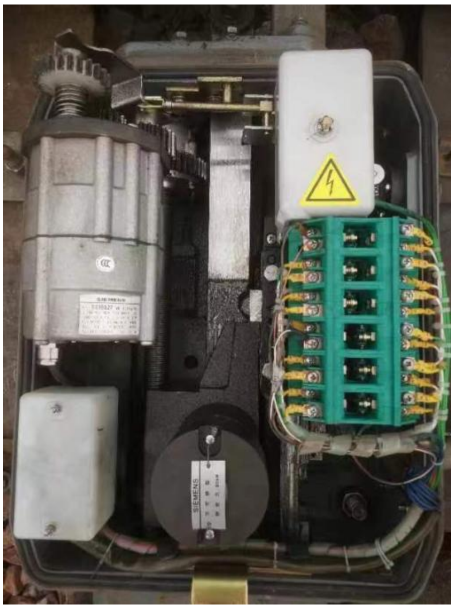

FIGURE 1. Schematic diagram of the internal structure of S700K turnout machine

3. Related Theories and Algorithms.

3.1. Improved multi-scale dispersion entropy.

Dispersion entropy is a measure of the complexity of the time series, and has been widely used in recent years in the extraction of vibration signal features of mechanical equipment due to its fast calculation speed and small impact by sudden change signals, and its calculation process is as follows.

1) For a given original signal sequence $\boldsymbol{x} = \{x_i, i = 1, 2, \ldots, n\}$ of length n, it is transformed into $\boldsymbol{y} = \{y_i, i = 1, 2, \ldots, n\}$ by calculating the normal cumulative distribution function (NCDF). Subsequently, a linear transformation is applied to obtaining $\boldsymbol{z} = \{z_i, i = 1, 2, \ldots, n\}$. The calculation formulas are as follows:

$$y_i = \frac{1}{\sigma\sqrt{2\pi}} \int_{-\infty}^{x_i} e^{\frac{-(t-u)^2}{2\sigma^2}} dt \tag{2}$$

$$z_i = round(c * y_i + 0.5) \tag{3}$$

where σ and u represent the standard deviation and mean of sequence $\boldsymbol{x}$, respectively, c denotes the number of classes, $y_i \in (0, 1)$, and $round()$ represents the rounding function. Through two transformations, $\boldsymbol{x}$ is mapped to the integer range $[1, 2, \ldots, c]$.

2) Under the time delay of τ and embedding dimension of m, the sequence $\boldsymbol{z}$ is reconstructed in the phase space, resulting in $K = n - (m-1)\tau$ reconstructed components of length m.

$$\begin{cases} \boldsymbol{v}_1 = \left\{z_1, z_{1+\tau}, \ldots, z_{1+(m-1)\tau}\right\} \\ \boldsymbol{v}_2 = \left\{z_2, z_{2+\tau}, \ldots, z_{2+(m-1)\tau}\right\} \\ \vdots \\ \boldsymbol{v}_K = \left\{z_K, z_{K+\tau}, \ldots, z_{K+(m-1)\tau}\right\} \end{cases} \tag{4}$$

3) For an individual reconstructed component $\boldsymbol{v}_i$, as each element takes integer values from 1 to c, there are a total of m possible combinations. And the possible combinations of permutations in the reconstructed component are noted as dispersion patterns. Assuming that across all reconstructed components, there are a total of l different dispersion patterns observed, the probability of each dispersion pattern π_i occurring is calculated as follows:

$$p(\pi_i) = \frac{num(\pi_i)}{K} \tag{5}$$

4) The dispersion entropy (DE) value of the original signal sequence is calculated based on the probabilities of the dispersion patterns.

$$\mathrm{DE}(\boldsymbol{x}, c, m, \tau) = -\sum_{i=1}^{l} p(\pi_i) \ln(p(\pi_i)) \tag{6}$$

Multi-scale dispersion entropy (MDE) is based on which the original signal sequence is segmented at different scales by coarse granulation, and then the dispersion entropy values at different scales are calculated to form multi-scale dispersion entropy. For the signal sequence $\boldsymbol{x} = \{x_i, i = 1, 2, \ldots, n\}$, sequence $\boldsymbol{x}^s = \{x_i^s, i = 1, 2, \ldots, [n/s]\}$ is obtained by coarse granulation at time scale s. The calculation formula is as follows:

$$x_i^s = \frac{1}{s} \sum_{j=(i-1)s+1}^{is} x_j \tag{7}$$

$$\mathrm{MDE}\left(\boldsymbol{x}, c, m, \tau, s\right) = \mathrm{DE}\left(\boldsymbol{x}^s, c, m, \tau\right) \tag{8}$$

Due to the coarse granulation process starting from the beginning of the signal sequence, it tends to overlook the information at the end of the signal. As the time scale increases, more information is lost from the signal's end, leading to insufficient feature extraction.

This paper proposes an improved multi-scale dispersion entropy (IMDE) method to address this issue. Instead of the traditional coarse granulation approach, a sliding time-shift averaging method is employed on the original signal sequence $\boldsymbol{x}$ at the same time scale s, generating multiple different sequences $\{\boldsymbol{g}^i, i = 1, 2, \ldots, s\}$. The dispersion entropy of each sequence is computed and averaged to obtain the dispersion entropy value at that time scale. The calculation formula is as follows:

$$g_i^m = \frac{1}{s} \sum_{j=(i-1)s+m}^{is+m-1} x_j \tag{9}$$

$$\text{IMDE}(\boldsymbol{x}, c, m, \tau, s) = \frac{1}{s} \sum_{m=1}^{s} \text{DE}\left(\boldsymbol{g}^m, c, m, \tau\right) \tag{10}$$

3.2. **Stack auto-encoder.** Auto-encoder is a widely applied self-supervised learning model in recent years, and its structure is divided into two parts: encoder and decoder. The encoder part extracts informative low-dimensional representations through dimensionality reduction, while the decoder part aims to reconstruct the data from the low-dimensional representations. By training the model's ability to reconstruct, the low-dimensional representations can capture the essence of the original data. The process can be described as follows.

The typical structure of stack auto-encoder is shown in Figure 2. The original data $\boldsymbol{x} = \{x_1, x_2, \ldots, x_n\}$ is progressively reduced to a lower-dimensional representation $\boldsymbol{h} = \{h_1, h_2, \ldots, h_i\}$, through successive layers. Subsequently, the lower-dimensional representation $\boldsymbol{h}$ is upsampled to reconstruct the data resulting in $\tilde{\boldsymbol{x}} = \{\tilde{x}_1, \tilde{x}_2, \ldots, \tilde{x}_s\}$. The model is trained by minimizing the mean squared error between $\boldsymbol{x}$ and $\tilde{\boldsymbol{x}}$. Finally, the representation $\boldsymbol{h}$ serves as the feature representation of the original signal. The computation formula for the neurons between adjacent layers is as follows:

$$\boldsymbol{y} = f(W\bar{x} + b) \tag{11}$$

where $\bar{x}$ represents the output of the neurons in the previous layer, $\boldsymbol{y}$ denotes the output of the neurons in the current layer, W represents the weight matrix, b denotes the bias, and f denotes the activation function.

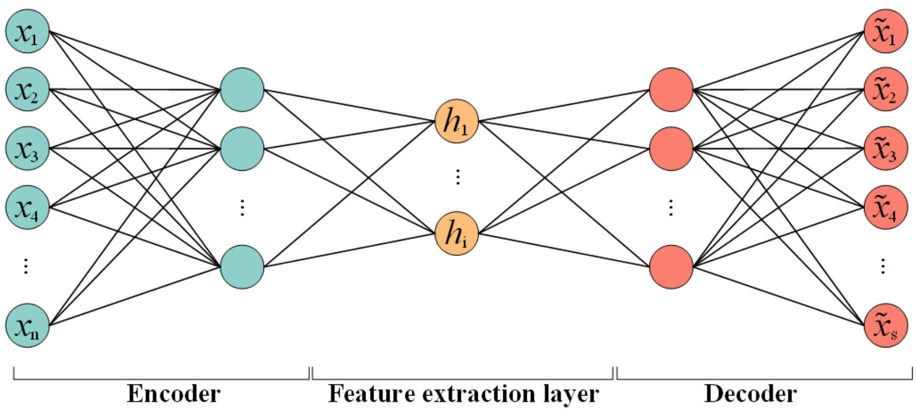

FIGURE 2. Stack auto-encoder diagram

3.3. **Gaussian process regression.** The theoretical foundation of Gaussian process regression (GPR) is Bayesian linear regression, which uses prior probability to compute the posterior probability. For a given training sample set $T = \{(x_i, y_i)|i = 1, 2, \ldots, n\}$ with n samples, where $x_i \in \mathbb{R}^k$ represents the input vector of the model and $y_i \in \mathbb{R}$ represents the output vector with Gaussian white noise, denoted by $\boldsymbol{X}$ and $\boldsymbol{Y}$ as the sets of input and output vectors respectively, the relationship between the input and output can be described as follows:

$$\boldsymbol{y} = f(\boldsymbol{x}) + \varepsilon \tag{12}$$

where f is the nonlinear mapping and ε is the Gaussian white noise obeying $N \sim (0, \sigma^2)$. In practical computations, a Gaussian process prior is imposed on $f(\boldsymbol{x})$, yielding the following expression:

$$f(\boldsymbol{x}) \sim GP\left(m(\boldsymbol{x}), k\left(\boldsymbol{x}, \boldsymbol{x'}\right)\right) \tag{13}$$

In this equation, $m(\boldsymbol{x})$ represents the mean function, and $k(\boldsymbol{x}, \boldsymbol{x'})$ denotes the covariance function, also known as the kernel function. In Gaussian process regression, the mean function is commonly set to 0, and the Gaussian kernel is often chosen as the kernel function. Its expression is given by

$$k\left(\boldsymbol{x}, \boldsymbol{x'}\right) = \sigma_f^2 \exp\left(-\frac{\left(\boldsymbol{x} - \boldsymbol{x'}\right)^2}{2l^2}\right) \tag{14}$$

Then the prior distribution of $\boldsymbol{Y}$ can be obtained as follows:

$$\boldsymbol{Y} \sim N\left(0, K(\boldsymbol{X}, \boldsymbol{X}) + \sigma_n^2 \boldsymbol{I}_n\right) \tag{15}$$

For a test value $\boldsymbol{x}^*$ and its corresponding predicted output y^*, the joint prior distribution of $\boldsymbol{Y}$ and y^* can be obtained as follows:

$$\left[\begin{array}{c} \boldsymbol{Y} \\ y^* \end{array}\right] \sim N\left[0, \begin{array}{cc} K\left(\boldsymbol{X}, \boldsymbol{X}\right) + \sigma_n^2 \boldsymbol{I}_n & K\left(\boldsymbol{X}, \boldsymbol{x}^*\right) \\ K\left(\boldsymbol{x}^*, \boldsymbol{X}\right) & k\left(\boldsymbol{x}^*, \boldsymbol{x}^*\right) \end{array}\right] \tag{16}$$

According to Bayes theorem, the posterior distribution of y^* can be calculated as follows:

$$y^* \left| \boldsymbol{X}, \boldsymbol{Y}, \boldsymbol{x}^* \sim N\left(u^*, \sigma^*\right)\right. \tag{17}$$

$$u^* = K\left(\boldsymbol{x}^*, \boldsymbol{X}\right)\left[K\left(\boldsymbol{X}, \boldsymbol{X}\right) + \sigma_n^2 \boldsymbol{I}\right]^{-1} \boldsymbol{Y} \tag{18}$$

$$\sigma^* = k\left(\boldsymbol{x}^*, \boldsymbol{x}^*\right) - K\left(\boldsymbol{x}^*, \boldsymbol{X}\right)\left[K\left(\boldsymbol{X}, \boldsymbol{X}\right) + \sigma_n^2 \boldsymbol{I}_n\right]^{-1} K\left(\boldsymbol{X}, \boldsymbol{x}^*\right) \tag{19}$$

where u^* and σ^* represent the mean and variance of the predicted output, respectively. Typically, the mean u^* is considered as the output for regression prediction.

4. **Predictive Method for Health State of S700K Turnout Machine.** S700K turnout machine, as a crucial actuator in high-speed railway turnout operations, significantly influences the safety and reliability of train travel. Current research on the S700K turnout machine primarily focuses on fault analysis, aiming to identify differences between normal operation and various fault states to ensure proper functioning and maintenance. However, this approach falls short in fault prevention, as it relies on limited fault data and requires extensive expert knowledge for analysis. To address this issue, this paper proposes a novel approach based on the full-cycle operational data of S700K turnouts machine, employing the IMDE-SAE algorithm to extract health indicators with degradation trends. Subsequently, the Gaussian process regression model is applied to predicting the health state of the turnouts machine. The workflow shown in Figure 3 is outlined as follows.

4.1. **Feature vector extraction.** In this study, we select all the power curve data captured by on-site microcomputer monitoring systems, ranging from normal to faulty states of the S700K turnouts. The IMDE method proposed in this paper is employed to extract meaningful features from the data. The IMDE approach addresses the information loss issue encountered in traditional coarse granulation processes by constructing multiple

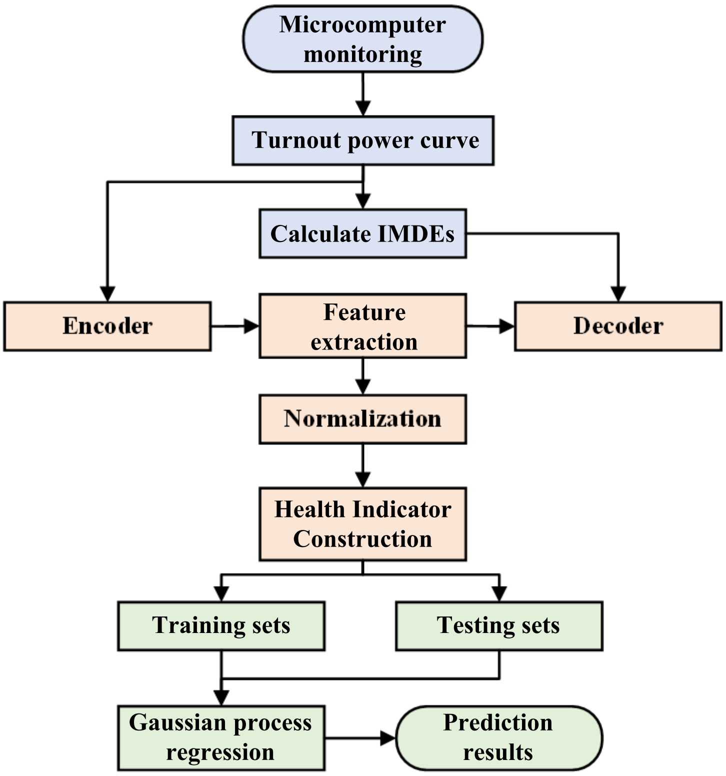

FIGURE 3. Turnout machine health state prediction flow chart

reconstruction sequences. Additionally, this paper determines the dimension of the time scale according to the changing trend of MDE, and selects the IMDE value with more characterization ability to construct the turnout machine power curve feature vector.

4.2. **Health indicators construction.** To analyze the turnout power curves, a stack auto-encoder (SAE) is constructed in this paper. The normalized power curve data is utilized as the input to the encoder of the SAE, while the IMDE feature vector is employed as the corresponding label for the decoder. By training the dimensionality reduction and reconstruction ability of the model, a one-dimensional health indicator is obtained. Subsequently, the health indicator is normalized and constrained within the range of 0 to 1 to facilitate further analysis.

4.3. **Health state prediction.** The constructed health indicators are split into training and testing sets, and the GPR model is trained and validated using these sets. This approach enables the regression prediction of the turnout machine health indicator, facilitating the assessment of turnout machine health conditions.

5. Method Validation and Analysis.

5.1. **Data acquisition.** To validate the effectiveness of the proposed method, a power curve dataset from the microcomputer monitoring system was selected from a specific S700K turnout machine at a station of Lanzhou Railway Bureau. The dataset consists of 340 consecutive operations of the turnout machine from normal to failure states, with a sampling interval of 40 ms. The sampling time of the turnout machine in normal operation is usually within 7 s. Figure 4 illustrates the power curve of the S700K turnout machine during normal operation, which can be characterized by three main stages: unlocking, transition and locking.

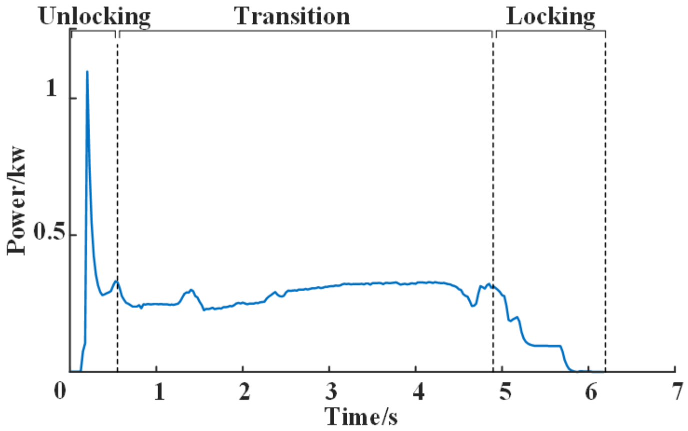

Figure 4. Power curve of S700K turnout machine under normal operation state

During the unlocking stage, the power curve exhibits a transient peak due to the initial zero velocity of the motor and the significant resistance encountered during the unlocking process. Subsequently, as the turnout completes the unlocking process, it enters the transition stage. At this stage, the turnout smoothly glides along the sliding bed with the point rail being pushed or pulled, resulting in a gradual decrease and relatively gentle amplitude in the power curve. Once the point rail tightly aligns with the stock rail, indicating the completion of the turnout transition, the turnout enters the locking stage. In this stage, the turnout control circuit is disconnected, and the power curve amplitude gradually diminishes to zero.

5.2. **Feature vector extraction.** The IMDE of the turnout machine power curve is calculated according to the steps in Section 3.1, where the parameters to be set are number of classes c, embedding dimension m, time delay τ, and time scale s. The number of classes c is typically chosen as an integer between 5 and 7. The embedding dimension m determines the number of dispersion patterns, which is generally 2 or 3 to avoid excessive dispersion of patterns. The time delay τ is commonly set to 1. The time scale s is related to the dimensionality of the extracted feature vectors, and generally should not be too large or too small. By adjusting and referring to the parameter selection in [16], the IMDE parameters are set as follows: $m = 2$, $c = 5$, $\tau = 1$.

Figure 5 shows the MDE, IMDE, and MPE values of the power curve of the S700K turnout machine at different time scales ranging from 1 to 20. As the time scale increases (denoted as IMDEx when s equals x), the IMDE exhibits a smooth decreasing trend, while the MDE and MPE show little noticeable change. This observation indicates that the IMDE can characterize more information in comparison. When the time scale $s = 15$, the MDE and IMDE values are approximately equal. Subsequently, both measures remain consistent and show slight variation. Therefore, in this paper, we select the IMDE1 to IMDE15, which possess deeper information, as the feature vectors for analysis.

Figure 6 shows the IMDE distribution of the turnout machine for the full operating cycle with the assumed time scale $s = 2$. It can be observed that as the number of transitions increases, the IMDE2 value shows an increasing trend. However, significant fluctuations and a lack of clear degradation trend are present. Using a single-scale IMDE value as the health indicator for the turnout machine may not effectively reflect its degradation process. To address this issue, this paper constructs a 15-dimensional feature vector (IMDE1$\sim$IMDE15) and utilizes it as the decoding labels for the stack auto-encoder. By integrating the temporal features of the original signal data, it extracts health indicators that exhibit degradation tendencies.

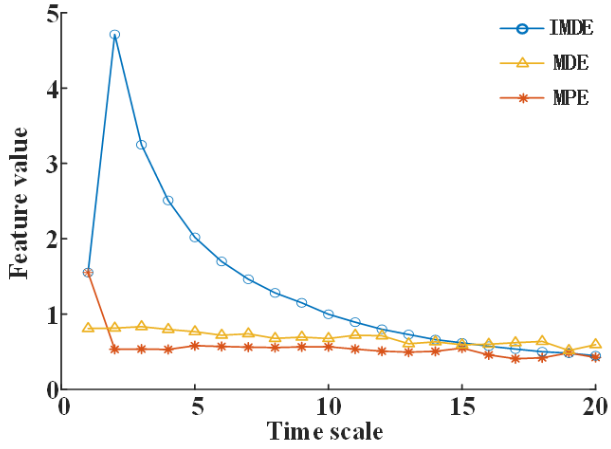

FIGURE 5. IMDE, MDE and MPE values at different time scales

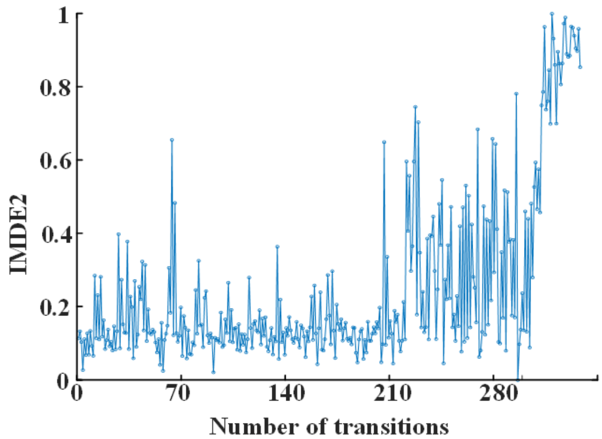

FIGURE 6. The IMDE2 distribution of the turnout machine under the full operating cycle

5.3. **Health indicators construction.** In this paper, the stack auto-encoder is built with the Matlab platform, and two fully connected layers are used for both the encoder and decoder. The normalized power data of the turnout machine is used as input for the decoder, which is reduced to one dimension, and then reconstructed into a 15-dimensional feature vector. During the training process, the learning rate is set to 0.01, and the Adam optimization algorithm is selected as the parameter update strategy. The batch size is set to 20. The mean squared error (MSE) measures the difference between the original and reconstructed data, serving as the loss function for parameter updates. The calculation formula for MSE is as follows:

$$\mathrm{MSE} = \sum_{i=1}^{n} \left(y_i - \tilde{y}_i\right)^2 \Big/ n \tag{20}$$

TABLE 1. Stack auto-encoder model parameters

Parameters	Number of neurons	Learning rate	Batch size	Training rounds	Optimizer	Loss function
Value	249, 10, 1, 10, 15	0.01	20	100	Adam	MSE

The trained stack auto-encoder is used as a feature extractor by removing its decoder part and obtaining the one-dimensional features from its feature extraction layer as output. In this paper, the health indicator of the turnout machine is set within the range of 0 to 1, where a value closer to 0 indicates a poorer health condition of the turnout machine. Since the feature values do not fall within this interval, normalization is applied to bringing them into the desired range. The specific formula for normalization is as follows:

$$\mathrm{HI} = \frac{p - p_{\min}}{p_{\max} - p_{\min}} \tag{21}$$

where $p_{\max}$ and $p_{\min}$ are the maximum and minimum values of this one-dimensional feature, respectively, and the HI value is ensured to be within the range of 0 to 1 by normalization, which serves as the health indicator for the turnout machine. Through communication with the on-site staff, it has been determined that the power curve of the turnout machine can reflect its performance degradation. When the S700K turnout machine operates normally, the power curve remains relatively stable. However, as time passes and the mechanical structure of the turnout machine ages, fluctuations appear in the power curve [9]. As shown in Figure 7, an increasing HI value is associated with a convex trend in the amplitude of the power curve, indicating a gradual deterioration in the health state of the turnout machine. This demonstrates that the constructed health indicator in this paper can, to some extent, reflect the degradation trend of the turnout machine.

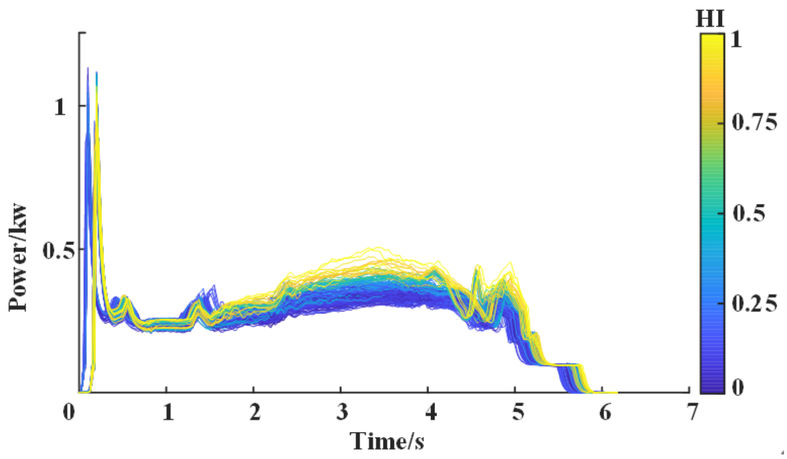

FIGURE 7. (color online) Turnout machine health indicator chart

The distribution of health indicators for the turnout machine is illustrated in Figure 8. The blue curve is the calculated value of the health indicators, which is smoothed to get the red curve to reflect the general trend. It can be observed that the turnout machine operates in a stable state most of the time, exhibiting relatively smooth and minimal fluctuations in the health indicators. The operational cycle can be divided into three stages. The first stage spans from the 1st to the 219th transition of the turnout machine, during which the health indicators remain below 0.2 with minor fluctuations. The second stage encompasses the 220th to the 298th transition, where a significant mutation occurs in the health indicators. Although there are some instances of regression during this stage, the overall level notably increases. In the third stage, the health indicators exhibit a significant increase and remain consistently high, indicating a clear degradation in the turnout machine's health state. In this paper, the initial indicator value of 0.477 during the third stage is chosen as the threshold for early warning. It is considered the point when

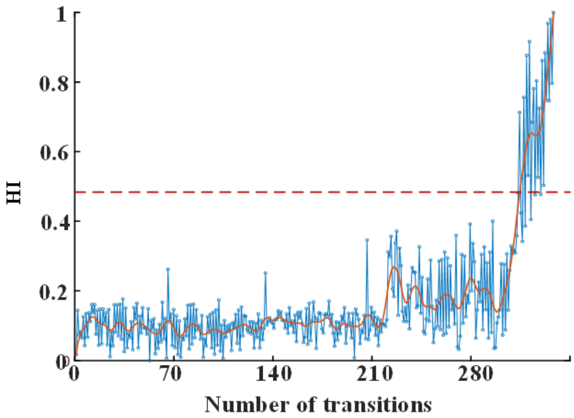

FIGURE 8. Distribution of turnout machine health indicators

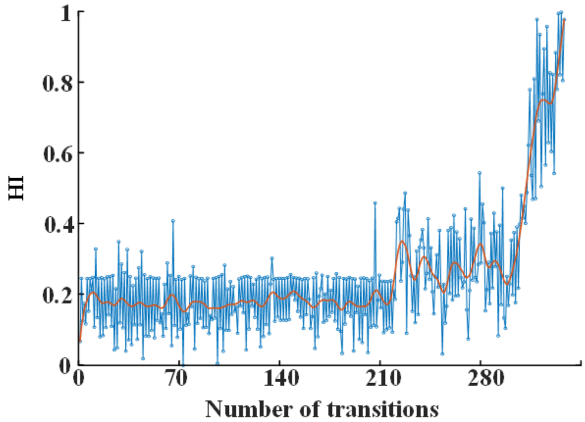

(a) MDE-SAE

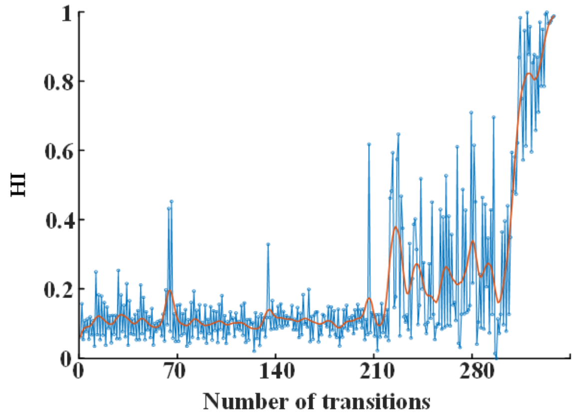

(b) IMDE-KPCA

FIGURE 9. Comparison of health indicators of turnout machines

TABLE 2. Comparison of health indicators of different methods

Evaluation indicators	IMDE-SAE	MDE-SAE	IMDE-KPCA
Std	0.0484	0.0812	0.0660
Cor	0.8630	0.8485	0.8616

the operational state of the turnout machine changes, and its health condition starts to deteriorate.

To verify the effectiveness of the health indicator construction method of the turnout machine proposed in this paper, two methods of health indicator construction, MDE-SAE and IMDE-KPCA, were compared. The stability of the HI during the first stage of the smooth operation of the turnout machine was evaluated using the standard deviation (Std), while the correlation (Cor) was used to measure the relationship between HI and the number of transitions during the third stage of significant degradation of the turnout machine. The results of different health indicators construction methods are shown in Figure 9. The blue and red curves indicate the specific calculated value of HI and the trend after smoothing it, respectively. The experimental results are shown in Table 2, indicating that the IMDE-SAE method proposed in this paper effectively utilizes the multi-scale information from the power curve of the turnout machine. The resulting HI is smoother and exhibits better degradation representation than the alternative approach.

5.4. **Health state prediction.** The constructed health indicator data for the turnout machine in this paper were divided into training and testing sets in a ratio of 0.8 : 0.2. The testing set was used to validate the trained GPR model. Two evaluation metrics, Root Mean Square Error (RMSE) and Coefficient of Determination (R^2) were employed to assess the prediction accuracy of the model. RMSE quantifies the difference between predicted and actual values, with smaller values indicating higher prediction accuracy. R^2 represents the goodness of fit between predicted and actual values, with larger values indicating a better fit. The formula for both is shown in Equations (22) and (23). Additionally, this paper compared three commonly used time series prediction models, BP, LSTM and SVR. Figure 10 shows the comparison results of different time series prediction models. Table 3 reveals that the GPR model outperforms these models in terms of prediction accuracy and provides a better fit to the data.

$$\mathrm{RMSE} = \sqrt{\sum_{i=1}^{n} (y_i - \tilde{y}_i)^2 \Big/ n} \tag{22}$$

$$\mathrm{R}^2 = 1 - \frac{\sum_{i=1}^{n} (y_i - \tilde{y}_i)^2}{\sum_{i=1}^{n} (y_i - \bar{y}_i)^2} \tag{23}$$

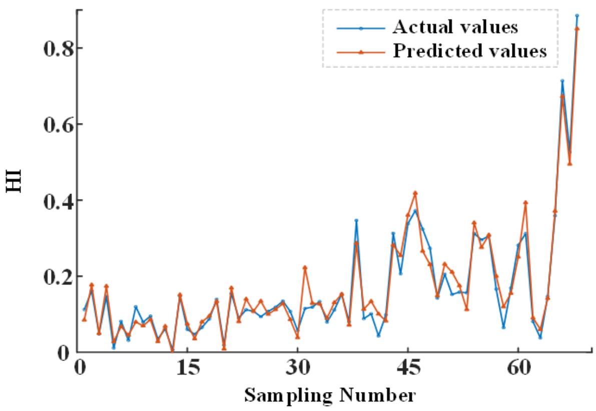

(a) GPR

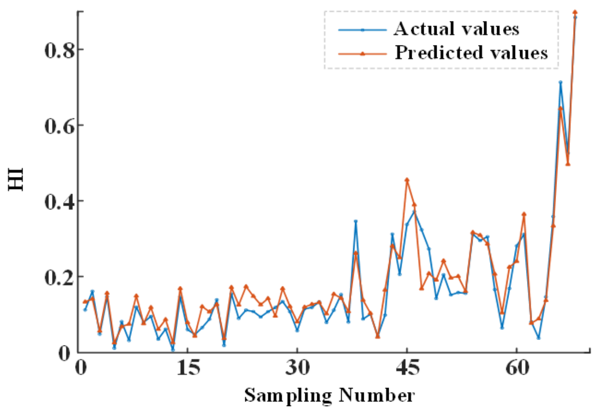

(b) BP

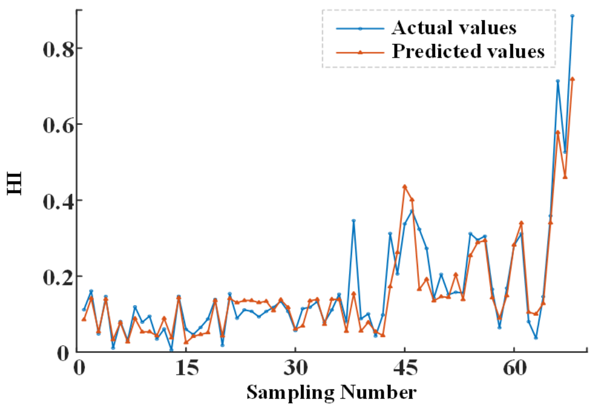

(c) LSTM

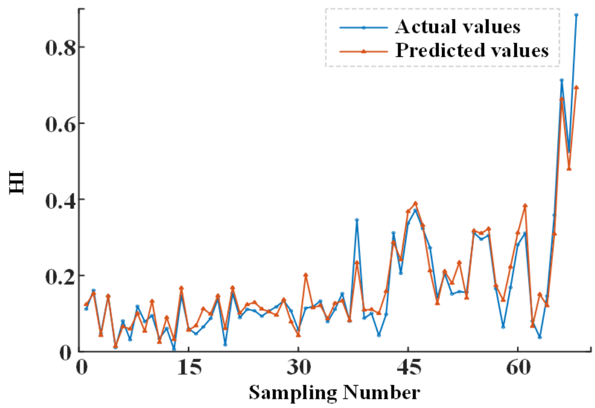

(d) SVR

FIGURE 10. Health state prediction results of turnout machine

TABLE 3. Comparison of health state prediction results of turnout machine

Evaluation Indicators	GPR	BP	LSTM	SVR
RMSE	0.0310	0.0410	0.0534	0.0434
R^2	0.9585	0.9272	0.8765	0.9185

6. **Conclusions.** This paper proposes an improved method for multi-scale dispersion entropy, which avoids the loss of information at the end of the original signal during the multi-scale coarse granulation. Two feature extraction algorithms are compared: traditional multi-scale dispersion entropy and multi-scale permutation entropy. The results demonstrate that the improved multi-scale dispersion entropy exhibits superior representation capabilities for feature extraction from turnout machine power curve data.

In this paper, a stack auto-encoder is used for turnout machine health indicators extraction, considering the original information of the power curve with improved multi-scale scattering entropy features, and the obtained health indicators have better characterization ability for the degradation process of the turnout machine.

Gaussian process regression (GPR) is employed to perform regression learning on the power curve and health indicators of turnout machines, and three time series regression prediction models, BP, LSTM and SVR, are compared. The experimental results show that GPR has superior prediction accuracy and fitting ability in predicting the health state of turnout machines.

At present, the research on preventive repair of turnout machine is still a popular direction. In the future research, we hope to apply the knowledge graph and other data models to the research related to the intelligent operation and maintenance of turnout machine, so that the potential turnout machine failure data and related expert knowledge can be effectively utilized.

Acknowledgment. This work is partially supported by The National Natural Science Foundation of China (52162050) and The Opening Foundation of Key Laboratory of Opto-technology and Intelligent Control (Lanzhou Jiaotong University). The authors also gratefully acknowledge the helpful comments and suggestions of the reviewers, which have improved the presentation.

REFERENCES

[1] Z. Zhong, T. Tang and F. Wang, Research on fault feature extraction and diagnosis of railway switches based on PLSA and SVM, *Journal of the China Railway Society*, vol.40, no.7, pp.80-87, 2018.

[2] W. Wei, X. Zhang and L. Yang, Full-cycle state evaluation of S700K switch machine based on residual network and fuzzy clustering, *International Journal of Innovative Computing, Information and Control*, vol.18, no.4, pp.1203-1216, 2022.

[3] W. Wei, Z. Li and X. Wu, Running state diagnosis algorithm of S700K switch machine based on time-domain characteristics of power curve and variational modal decomposition, *China Railway Science*, vol.43, no.3, pp.144-154, 2022.

[4] W. Ji et al., An intelligent fault diagnosis method based on curve segmentation and SVM for rail transit turnout, *Journal of Intelligent and Fuzzy Systems*, vol.41, no.3, pp.4275-4285, 2021.

[5] D. Ou, Y. Ji, R. Zhang and H. Liu, An online classification method for fault diagnosis of railway turnouts, *Sensors (Switzerland)*, vol.20, no.16, pp.1-16, 2020.

[6] Z. Zhong, J. Chen, T. Tang, T. Xu and F. Wang, SVDD-based research on railway-turnout fault detection and health assessment, *Journal of Southwest Jiaotong University*, vol.53, no.4, pp.842-849, 2018.

[7] W. Wei, Z. Li, X. Wu and L. Gao, Running state assessment of S700K switch machine based on fuzzy clustering algorithm, *Journal of the China Railway Society*, vol.44, no.4, pp.74-81, 2022.

[8] X. Wu and X. Chu, Research on division of degradation stage of turnout equipment based on wavelet packet decomposition and GG fuzzy clustering, *Journal of the China Railway Society*, vol.44, no.1, pp.79-85, 2022.

[9] Y. Zhang, D. Zhang, N. Yang and Z. Wei, Degradation state recognition method of switch machine based on CEEMDAN and KFCM clustering, *China Railway Science*, vol.44, no.1, pp.194-201, 2023.

[10] Y. S. Zheng, W. M. Chen, Y. N. Zhang and D. Y. Bai, Prediction of the remaining useful life of a switch machine, based on multi-source data, *Sustainability*, vol.14, no.21, 14517, 2022.

[11] C. Chen, T. H. Xu, G. Wang and B. Li, Railway turnout system RUL prediction based on feature fusion and genetic programming, *Measurement*, vol.151, 107162, 2020.

[12] V. Atamuradov, K. Medjaher, F. Camci, P. Dersin and N. Zerhouni, Railway point machine prognostics based on feature fusion and health state assessment, *IEEE Transactions on Instrumentation and Measurement*, vol.68, no.8, pp.2691-2704, 2019.

[13] L. Gao, Q. Xu, F. Li, J. Yang, J. Meng and S. Yang, Research on degradation state of turnout equipment based on SOM-BP hybrid neural network, *China Railway Science*, vol.41, no.3, pp.50-58, 2020.

[14] H. Yin, Y. Liang and C. Wang, Health condition assessment of point machine based on a deep GRU model, *Journal of the China Railway Society*, vol.43, no.11, pp.88-96, 2021.

[15] Y. Zheng, D. Bai and Y. Wang, Research on turnout health state assessment and fault detection method based on similarity, *Journal of Railway Science and Engineering*, vol.18, no.4, pp.877-884, 2021.

[16] M. Rostaghi and H. Azami, Dispersion entropy: A measure for time-series analysis, *IEEE Signal Processing Letters*, vol.23, no.5, pp.610-614, 2016.

[17] Z. Zhang and G. Fu, Bearing fault detection based on improved multiscale dispersion entropy and single value classification, *IEEE Sensors Journal*, vol.22, no.16, pp.15825-15833, 2022.

[18] P. Wang, L. Deng, B. Tang and Y. Han, Degradation trend prediction of rolling bearing based on auto-encoder and GRU neural network, *Journal of Vibration and Shock*, vol.39, no.17, pp.106-111+133, 2020.

[19] S. Wang, W. Zhang, G. Zheng, X. Li and Y. Zhao, Fault diagnosis of wind turbine generator with stacked noise reduction autoencoder based on group normalization, *Energy Engineering: Journal of the Association of Energy Engineering*, vol.119, no.6, pp.2431-2445, 2022.

[20] Z.-K. He, G.-B. Liu, X.-J. Zhao and M.-H. Wang, Overview of Gaussian process regression, *Control and Decision*, vol.28, no.8, pp.1121-1129+1137, 2013.

[21] J. Qin, D. Zheng, Y.-Q. Pei, Y. Lyu, Q.-P. Su and Y.-B. Wang, Prediction method of engine performance and emission based on PSO-GPR, *Journal of Jilin University (Engineering and Technology Edition)*, vol.52, no.7, pp.1489-1498, 2022.

Author Biography

Wenjun Wei graduated from Lanzhou Railway University, Lanzhou, China in 1995 with a B.Eng. degree in Industrial Electrical Automation, graduated from Lanzhou Jiaotong University, Lanzhou, China in 2001 with a M.Eng. degree in Traffic Information Engineering and Control, and graduated from Lanzhou Jiaotong University, Lanzhou, China in 2015 with a Ph.D. degree in Traffic Information Engineering. Dr. Wei is currently a full-time professor at the School of Automation and Electrical Engineering, Lanzhou Jiaotong University, China. He presided over 2 provincial and ministerial scientifific research projects, participated in 7 provincial projects, and obtained 4 invention patents and 3 utility model patents as a major member. He has published more than 20 academic papers, which have been indexed by EI, ISTP, and many domestic core journals. Research interests include multi-agent cooperative control and optimization, fault diagnosis of dynamic systems, and intelligent control theory and application.

Zheng Zhou obtained his B.Sc. degree in Rail Transit Signal from Lanzhou Jiaotong University, Jinzhou, China, in 2021, where he is currently pursuing the M.Sc. degree with Traffic Information Engineering and Control. His research interests include fault diagnosis and health state assessment of turnout machines.

Mengyu Li is currently pursuing his B.Sc. degree in Electrical Engineering from Lanzhou Jiaotong University, Jinzhou, China. His current research interests include intelligent operation and maintenance of electrical equipment.

Liben Yang received the B.Eng. degree in Communication Engineering from Kunming University of Science and Technology, China, 2000; the M.Sc. degree in Communication and Information System from Kunming University of Science and Technology, China, 2009; the Ph.D. degree in Control Science and Engineering, from Northwest University of Technology, China, 2017. Dr. Yang is currently a full-time associate professor at the School of Automation and Electrical Engineering, Lanzhou Jiaotong University, China. His main research interests include UAV control system, UAV autonomous intelligent control and intelligent control system based on reinforcement learning. He has published more than ten papers in well-known journals.